IEEE Access
Multidisciplinary | Rapid Review | Open Access Journal

Received May 23, 2019, accepted June 16, 2019, date of publication June 19, 2019, date of current version July 8, 2019.

Digital Object Identifier 10.1109/ACCESS.2019.2923632

Hand-Eye-Force Coordination of Acupuncture Robot

JIANBO SU, (Member, IEEE), YICHENG ZHU, AND MINGDE ZHU
Department of Automation, Shanghai Jiao Tong University, Shanghai 200240, China

Corresponding author: Jianbo Su (jbsu@sjtu.edu.cn)

This work was supported in part by the National Natural Science Foundation of China under Grant 61533012 and Grant 91748120.

ABSTRACT Acupoint is the intersection point of the main and collateral channels in a human body, through which energy circulates according to eastern philosophy. Acupuncture is the essential traditional Chinese method to treat disease by sticking the proper acupoints on the patient's body, having achieved a great therapeutic effect. Normally, acupuncture is mainly performed by skilled doctors of traditional Chinese medicine, which are far from enough for requirements. Hence it is natural to resort to robots to perform acupuncture work. There has no complete theoretical guidance for the development of an acupuncture robot so far. Thus, this paper digs out that acupuncture is essentially a visual servoing task with force constraints and the hand-eye-force coordination framework is first proposed. With the guidance of the framework, the acupuncture task is divided into three parts: hand-eye coordination, eye-force coordination, and hand-force coordination. The hand represents the end-effector of the acupuncture robot, the eye represents the visual sensor of the acupuncture robot, and the force represents the interaction between the acupuncture robot and the patient's body. The hand-eye coordination is the visual servoing control, eye-force coordination is to estimate force by vision, and hand-force coordination is the acupuncture operation with force constraint. The acupuncture task can be completed only when the three coordinations are well organized. The solutions are proposed for the three coordination tasks, which are finally validated by the experiments.

INDEX TERMS Acupuncture robot, hand-eye-force coordination.

I. INTRODUCTION

Acupuncture is an essential part of traditional Chinese medicine theory and has been used to treat human diseases for nearly three thousand years [1], [2]. With the continuous enrichment of acupuncture theory in recent years, good clinical effects have been achieved.

Acupuncture has been gradually recognized in the world, but its efficacy has been controversial. Hazzard believed that acupuncture was effective [3], while Taub accused acupuncture of being useless [4]. In 2010, acupuncture was successfully declared a human intangible cultural heritage, and Goldman et al. demonstrated the effectiveness of acupuncture [5]. This is simply because that the judgment of whether acupuncture is effective is subjective, which make it far from a widely accepted science for cure of disease [6].

With the help of the robot, the acupuncture work can be repeatable and objective. Besides, the basis for the quantitative analysis of acupuncture will be proposed, so as to make the acupuncture task more standardized. In addition, acupuncture robot brings much convenience to human beings, since it supports remote control and reduces the workload of doctors. Therefore, it is necessary to develop the acupuncture robot which can greatly promote the standardization of acupuncture to bring new solutions to the cure of diseases.

The associate editor coordinating the review of this manuscript and approving it for publication was Hui Xie.

II. RELATED WORK

In recent years, the development of surgical robot is rapid, the robot Da Vinci developed by Intuitive Surgical played an important role in Surgical work [7], [8]. ZEUS robot developed by Computer Motion [9], ROSA robot developed by Medtech [10], Magellan robot developed by Hansen Medical [11],and CardioArm robot from Carnegie Mellon University [12] played important roles in medicine. The development of these surgical robots provides important reference and hardware support for the realization of acupuncture robots.

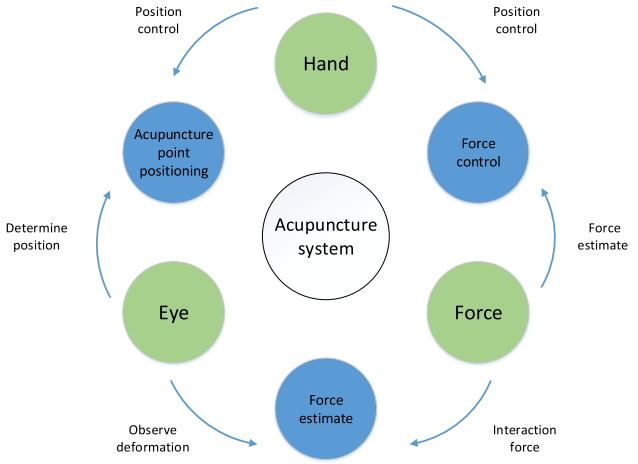

FIGURE 1. Hand-eye-force coordination system for acupuncture.

However, compared with these surgical robots, the development of acupuncture robots is almost blank at present. Wang yu et al. designed a mechanism for automatic needle feeding and needle changing [13]. The existing work is the simple grasping mechanisms for acupuncture needles and cannot accomplish acupuncture work. An acupuncture robot system needs to clarify the various operations of acupuncture, and find correct ways to complete the task of acupuncture. However, there is no systematic guidance on development of the acupuncture robot. This paper proposes a hand-eye-force coordination strategy and system development framework to implement the acupuncture robot.

III. SOLUTION

The process of acupuncture treatment can be divided into four stages: diagnosis, acupoint position, needling and needle withdrawing [14], [15]. The essential operation is the needling. During needling, doctors need to coordinate the hand, eye, and force. The eyes are used to find acupoints and guide the hands to reach the correct position for needling. The magnitude of force is the constraint condition of the hands in the process of needling. Only with the coordination of the three parts can doctors successfully complete the acupuncture task.

For the acupuncture robot, the hand is the end-effector which is used for holding and pricking needles, the eye is the visual sensor which is used to obtain the environmental information, and the force is the interaction between the needle and the patient which is a constraint condition. Through the analysis above, we summarize the work of acupuncture as the task of hand-eye-force coordination and then decompose hand-eye-force coordination into three parts: hand-eye coordination, eye-force coordination, and hand-force coordination. The relationship among them is shown in Fig. 1.

Hand-eye coordination is essentially a visual servoing task, which is to observe the position of acupoints and then control the end-effector to the target position. Eye-force coordination is to observe the deformation caused by the interaction of forces through vision, and then estimate the magnitude of the force. Hand-force coordination is a servoing control under the condition of force constraint, which means that the force should be strictly controlled in the process of acupuncture to prevent the needle from hitting the bone. To sum up, the robot with hand-eye-force coordination, has the ability to prick a specific point with a bounded force.

A. HAND-EYE COORDINATION OF ACUPUNCTURE ROBOT

Based on the analysis above, hand-eye coordination of acupuncture robot is essentially a visual servoing task. Visual servoing has eye-to-hand and eye-in-hand system structure [16]–[19]. Considering that the robot should be able to observe acupoints at a distance and have accuracy in acupoint positioning, the hand-eye coordination part adopts structure of eye-in-hand. When the camera is away from the target, the overall scene can be observed. When the camera gets close to the target, the local details can be observed to ensure the accuracy. The method to solve the visual servoing control are diverse. For example, Dean-Leon et al. used PID control [20], Piepmeier et al. used quasi-Newton method to estimate the image jacobian matrix [21], and Levine et al. used deep learning method [22]. Considering PID control in relatively simple, do not have to train the network, and the accuracy can meet the requirements, the PID method is adopted.

1) OBJECT IDENTIFICATION

In the hand-eye coordination part, the first step is to identify the acupoints. It is said that the acupoints in a human body can be recognized by infra-red detector. To simplify this task, a circular label is used to mark the acupoints, and the center of the circle represents the target location where the acupuncture is to be performed. To test the robustness of the system, we use the labels of other shapes represents interference. The entire process is described below. Firstly, we preprocess the image collected by the camera and carry out contour detection. Then, Hu invariant moment is used to distinguish the circular label from the non-circular label [23]. Finally, Kernel Correlation Filter algorithm is used to solve the problem of interference of multiple identical labels in the image [24]. So as the target label is manually selected, the object identification system can track the label to provide coordinate information for subsequent servoing control.

2) CONTROL STRATEGY

The goal of the whole control is to get the robot arm to the acupoint, which is reflected in the camera's field of view by placing the label in the center of the imaging plane with the specified size. To achieve this, a hierarchical control strategy is designed. The whole motion of the end-effector is decomposed into the motion parallel and perpendicular to the camera's imaging plane. When the camera in the distant place, the end-effector is controlled to do the parallel motion to let the label reach the center of the camera's imaging plane(i.e. the coarse adjustment), followed by the perpendicular motion

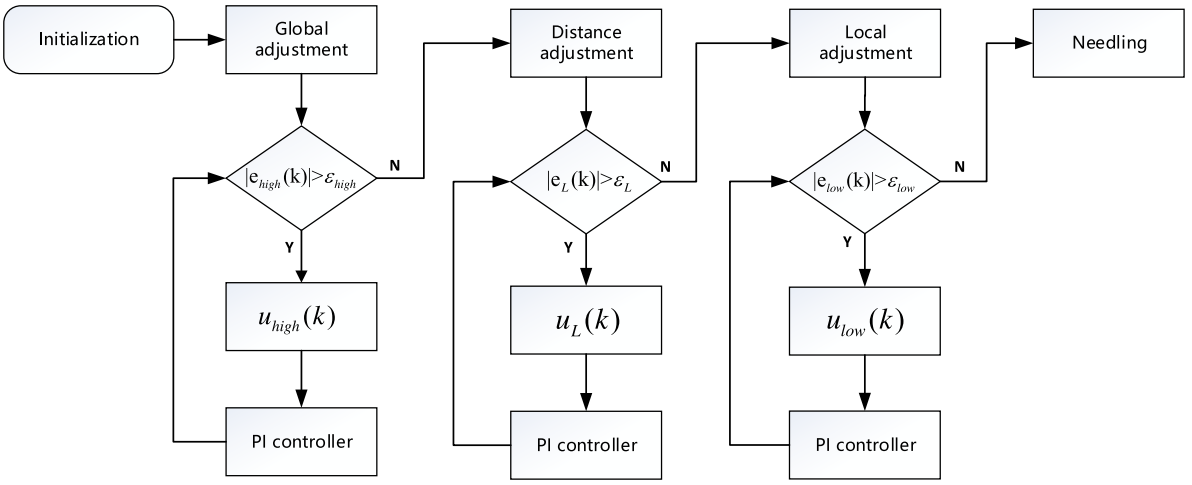

FIGURE 2. Flowchart of hierarchical control. $e_{high}(k)$ is the error in the coarse adjustment stage. $u_{high}(k)$ is the corresponding control quantity. ε_{high} is the error threshold set manually in the coarse adjustment stage. When $|e_{high}(k)| \leqslant \varepsilon_{high}$, it is considered that the coarse adjustment has been completed. $e_L(k)$ is the error in the distance adjustment stage. $u_L(k)$ is the corresponding control quantity. ε_L is the error threshold set manually in the distance adjustment. When $|e_L(k)| \leqslant \varepsilon_L$, it is considered that the distance adjustment has been completed. $e_{low}(k)$ is the error in the fine adjustment stage. $u_{low}(k)$ is the corresponding control quantity. ε_{low} is the error threshold set manually in the fine adjustment. When $|e_{low}(k)| \leqslant \varepsilon_{low}$, it is considered that the fine adjustment has been completed. Then the robot is ready to needle.

to let the size of the label in the camera's imaging plane reach the target(i.e. the distance adjustment). Finally, the end-effector is controlled to do the parallel motion(i.e. the fine adjustment), and the label is precisely adjusted to be in the center of the camera's imaging plane.

The goal of parallel motion is to control the pixel coordinates of the label at the center of the camera's imaging plane. To achieve this, we utilize strategy of the image Jacobian matrix. The image Jacobian matrix is the mapping relation from the image space to the robot motion space. Its definition is

$$\begin{cases} \dot{f} = J_i(q)\dot{q}, \\ J_i(q) = \begin{bmatrix} \dfrac{\partial K_1(q)}{\partial q_1} & \cdots & \dfrac{\partial K_1(q)}{\partial q_n} \\ \vdots & \ddots & \vdots \\ \dfrac{\partial K_m(q)}{\partial q_1} & \cdots & \dfrac{\partial K_m(q)}{\partial q_n} \end{bmatrix}_{m\times n}, \end{cases} \tag{1}$$

where $K_i \in R^m$ is the m-dimensional image feature collected by the robot. $q \in R^n$ is the position parameter of the robot in the task space. $J_i(q)$ is the image jacobian matrix. Most of the existing robot arms have complete capabilities of precise position control and path planning of the end-effector, so the task space can be defined as the coordinate system space of the robot base. The control quantity is the speed and the position of the end-effector.

When the end-effector moves parallel to the imaging plane of the camera, the image Jacobian matrix can be considered as a fixed value [25]. During initialization, the robot makes two linearly independent motions Δu_1 and Δu_2 parallel to the camera imaging plane. The position of the reaction in the camera's imaging plane is Δx and Δy. Then the two dimensional image Jacobian matrix can be estimated.

$$J_i = (\Delta x \ \Delta y)(\Delta u_1 \ \Delta u_2)^{-1}. \tag{2}$$

Let the image center point coordinate (target position) be $f_c = (u_c \ v_c)^T$. The coordinate of the current label center point in the imaging plane is $f(t)$. So the error is $e(t) = f(t) - f_c$. Simply using PI control law as an example, the controller is designed as

$$u(k+1) = J_i^{-1}(c_1 e(k) + c_2 \sum_{i=0}^{k} e(i)). \tag{3}$$

The goal of perpendicular motion is to make the size of the label in the camera's imaging plane(i.e. the pixel size of the label) as expected. According to the camera keyhole imaging model, we assume the true size of the label as R, the pixel size as r, the distance between the label and the camera as Z, and the camera focal length as f, then we have

$$\frac{R}{Z} = \frac{r}{f}. \tag{4}$$

That is, the pixel size of the label is inversely proportional to the distance between the label and the camera. Take the derivative of (4), then we have

$$dZ = -\frac{fR}{r}dr. \tag{5}$$

Suppose the target pixel size of the label is r_0, the current pixel size of the label is $r(t)$, and the error is $e(t) = r(t) - r_0$. PI control law is also adopted, and the controller is designed

$$u(k+1) = \frac{fR}{r(k)}(c_1 e(k) + c_2 \sum_{i=0}^{k} e(i)). \tag{6}$$

Fig. 2 shows the control diagram of the hierarchical control strategy mentioned above.

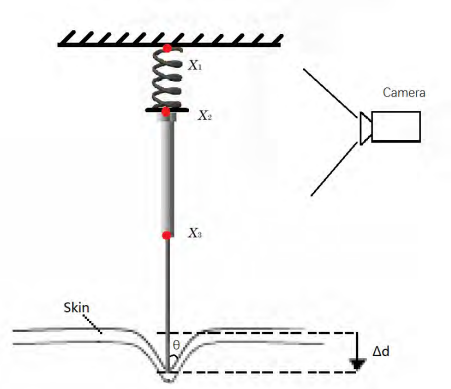

FIGURE 3. Conversion of the skin deformation.

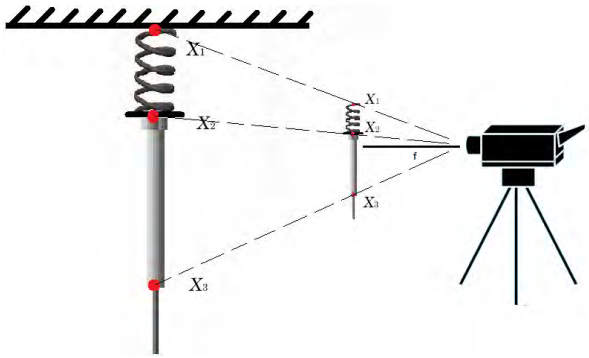

FIGURE 4. Methods to estimate the force.

B. EYE-FORCE COORDINATION OF ACUPUNCTURE ROBOT

In essence, the task of eye-force coordination is to estimate magnitude of the force during the process of acupuncture. The process of force interaction is accompanied by deformation, then the magnitude of the force can be estimated through visual observation of skin deformation, in order to alleviate the system configuration without force sensors.

1) THE TRANSFORMATION OF THE FORCE

It is difficult to observe skin deformation. According to the principle that force equal to reaction force, a special device is designed to transform the deformation of the skin into the deformation of the spring. The spring is installed above the needle, and the force is estimated by the deformation of the spring shown in Fig. 3.

When the spring does not exceed the elastic limit, the force on the skin can be figured out by

$$F = k(l_0 - \left|\overrightarrow{X_1X_2}\right|) + mg. \tag{7}$$

In (7), m is the total mass of the spring and needle, k is the spring's elastic coefficient, l_0 is the original length of the spring, and $\overrightarrow{X_1X_2}$ is the length of the spring after deformation. m, k, and l_0 can be measured in advance, so as long as the length of the spring after deformation is observed, the magnitude of the force can be estimated.

2) ESTIMATE OF THE FORCE

Three feature points are selected at the spring and needle ends, and the camera's imaging plane is parallel to the needle body, which ensures the spring and the needle have the same depth. Fig. 4 is a schematic diagram.

X_1, X_2, and X_3 are the coordinates in the world coordinate system. x_1, x_2, and x_3 are the coordinates in the pixel coordinate system. In the process of needling, the length of the spring will change, but the length of the needle will not change, which means $\overrightarrow{X_1X_2}$ will change while $\overrightarrow{X_2X_3}$ will not change. $\overrightarrow{X_1X_2}$ is what we want to estimate, while $\overrightarrow{X_2X_3}$ is the reference which can be measured in advance. Accordingly we have

$$|\overrightarrow{X_1X_2}| = \frac{|\overrightarrow{X_2X_3}|}{|\overrightarrow{x_2x_3}|} \cdot |\overrightarrow{x_1x_2}|. \tag{8}$$

By substituting (8) into (7), the magnitude of the force can be estimated

$$F = k(l_0 - \frac{|\overrightarrow{X_2X_3}|}{|\overrightarrow{x_2x_3}|} \cdot |\overrightarrow{x_1x_2}|) + mg. \tag{9}$$

C. HAND-FORCE COORDINATION OF ACUPUNCTURE ROBOT

Hand-force coordination is essentially a position control problem with force constraint. It is difficult to directly observe the state of the needle after inserted into the skin. So, it is impossible to judge whether the bone is hit by simple position control. Therefore, the force of the needle penetration should be restrained, and the needle should be withdrawn in time when the bone is hit, to avoid damage. That is to say, the problem of robot hand-force coordination is to constrain the force during position control.

Without loss of generality, it is assumed that the position control goal of the task is to make the robot move along the trajectory $A = \{a_1, a_2, \cdots, a_n\}$. At the intermediate point a_i of the trajectory, the magnitude of the force is F_i. The constraint is $F_i \leqslant F_{max}$. If the force exceeds the allowable upper limit F_{max} in the process of movement, it must be adjusted according to the requirements of the task so as to ensure safety.

1) FORCE DETECTION WITH DISCRETE FORCE CONVOLUTION

When the robot hit a bone, both the magnitude and the growth rate of the force will suddenly become greater. Discrete force convolution is used to construct a new evaluation standard, which takes both the magnitude and the growth rate of the force into consideration.

In a control system, force sampling is discrete. It is supposed that the sampling interval is t in a task with uniform velocity of v, and the force obtained at the time of nt is f_n, then we can get the discrete force sequence $f(n)$. The discrete

sequence $h(n)$, changing with $f(n)$ in real time, is constructed:

$$h(n) = f_n \begin{cases} \alpha & \text{if } 0 \leqslant n < k \\ -\alpha & \text{if } k \leqslant n < 2k \\ 0 & \text{others .} \end{cases} \tag{10}$$

In (10), $\alpha = \frac{\beta}{kv}, k \in N_+, \beta > 0$. Computing the discrete convolution of $f(n)$ and $h(n)$, we can get $F(n)$.

$$F(n) = f(n) * h(n) = \sum_{i=0}^{n} f(i)h(n-i). \tag{11}$$

Analyzing the convolution $F(n)$, we can see that $F(n)$ is essentially the product of the change rate and the magnitude of the force. The coefficient f_n is a good representation of the force; The average of discrete variables can largely suppress the noise interference; Coefficient $\frac{\beta}{v}$ can avoid the influence of change rate on the value of evaluation index. Therefore, it is very reasonable to use $F(n)$ as the criterion to distinguish whether the bone is hit or not.

2) CONTROL STRATEGY

In order to enable the robot to judge whether the needle held hit the bone or not, the threshold value of evaluation criteria $F(n)$ should be determined at first. According to the needling experiments without hitting the bone for many times, the maximum value of $F(n)$ (F_{max}) is collected as the standard to judge whether the needling process is normal. In the process of needling, the force is constantly detected and processed, the time series of the force is updated, and the discrete convolution function $F(n)$ is calculated. Then we compare it to threshold F_{max} in real time. If $F(n)$ is greater than the threshold F_{max}, the needling task is stopped immediately and the needling withdrawal operation is carried out to ensure safety.

IV. EXPERIMENTS AND ANALYSIS

The block diagram of the hand-eye-force coordination acupuncture robot system described is shown in Fig. 5. Hand-eye coordination system constantly collects acupoint information to ensure the smooth progress of automatic acupuncture. The eye-force coordination system estimates magnitude of the force in real time and calculates the discrete force convolution. The hand-force coordination system determines whether the bone is hit according to the discrete convolution of the force.

A. HAND-EYE COORDINATION

In the experiment, the model of the robot arm is UR3, the resolution of the color RGB camera is 720P, the sampling frequency of our camera system is 30Hz, and the needle holding device relative to the robot arm is shown in Fig. 6. The label of acupoints is a black circle with a diameter of 5mm, and other shapes are interference terms. There is no strict requirement for lighting conditions, just under normal fluorescent lamps.

The goal of hand-eye coordination is to locate the selected label and perform the needling. Firstly, we manually select

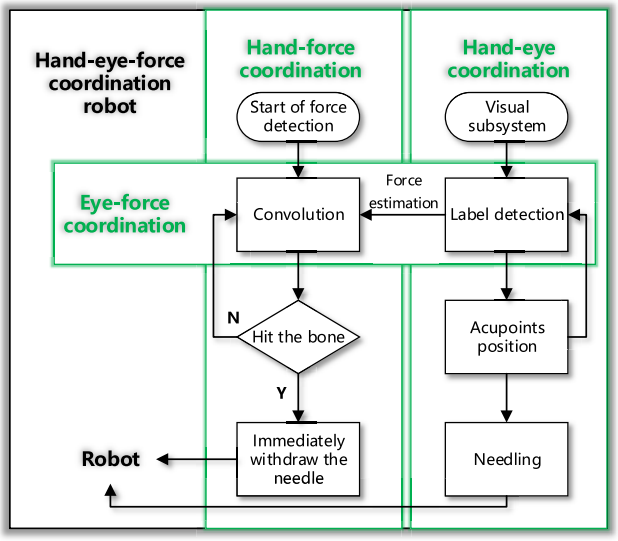

FIGURE 5. The block diagram of the hand-eye-force coordination acupuncture robot system.

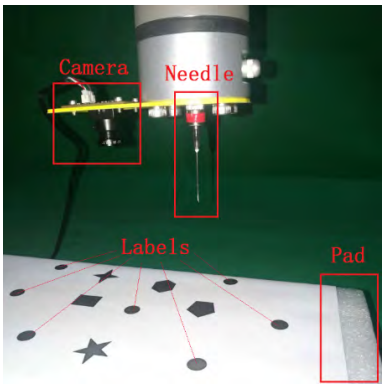

FIGURE 6. Introduction of hand-eye coordination experimental platform.

the label to track. Then the coarse adjustment is made to move the label close to the center of the screen, and the deviation less than 10 pixels can be considered as convergence. Then it comes to the distance adjustment stage. Adjust the distance to let radius equal to 50 pixels, and converge when the error is less than 1 pixel. In the fine adjustment stage. The label is adjusted in the center of the screen, with the error less than 1 pixel. The entire process is shown in Fig. 7, where you can see the needle is controlled to accurately insert into the previously selected label, with the accuracy shown in Table 1.

From Table 1, it can be seen that the pixel errors in all three directions are less than 1 pixel. Needling on the same label for many times, the furthest deviation from the center of the circle is less than 1.5mm, which meets the requirements of acupuncture accuracy.

B. EYE-FORCE COORDINATION

In the experiment, the position of the camera and the robotic arm is shown in Fig. 8. The force measuring device is $sf-400$

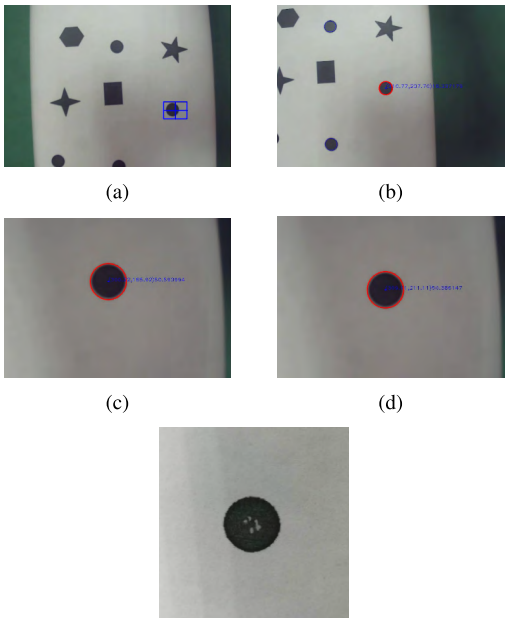

FIGURE 7. The entire process. (a) Select tag. (b) Coarse adjustment. (c) Distance adjustment. (d) Fine adjustment. (e) Needling.

TABLE 1. Pixel error of the final frame.

Number	X-error(Pix)	Y-error(Pix)	R-error(Pix)
1	0.435852	-0.11758	0.642914
2	0.196564	0.162354	0.337688
3	-0.06232	-0.30757	0.322517
4	0.362396	0.824127	0.365246
5	-0.60208	0.348465	-0.39809
6	0.179016	0.080246	0.311855
7	-0.67209	-0.01623	0.094536
8	-0.25940	-0.57520	-0.04482
9	-0.36469	0.475021	-0.01649
10	0.106781	0.243912	-0.2315
MAE	0.324118	0.315071	0.276566

pressure sensor with a precision of $1g$. We use red tape winding as the characteristic labels of the estimated force in the front of the end-effector. The distance between the lower two labels is $8.1mm$, and the distance between the upper two labels without pressing is $19.5mm$. The spring's elastic coefficient is $240N/m$, the variable of spring mounting shape is $2mm$, and the weight of spring and slider is $10g$.

The goal of eye-force coordination is to estimate the magnitude of the force. Through the analysis above, the calculation formula of force can be obtained by substituting the above parameters into (9):

$$F = 240 \times (0.0195 - \frac{0.0081 \times \sqrt{(u_1 - u_2)^2 + (v_1 - v_2)^2}}{\sqrt{(u_3 - u_2)^2 + (v_3 - v_2)^2}} + 0.002) + 0.098, \quad (12)$$

where (u_1, v_1), (u_2, v_2), (u_3, v_3) are pixel coordinates of three feature points from top to bottom. In the experiment we press

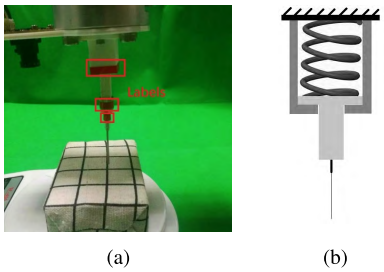

FIGURE 8. Introduction of eye-force coordination experimental platform. (a) Material object. (b) Model.

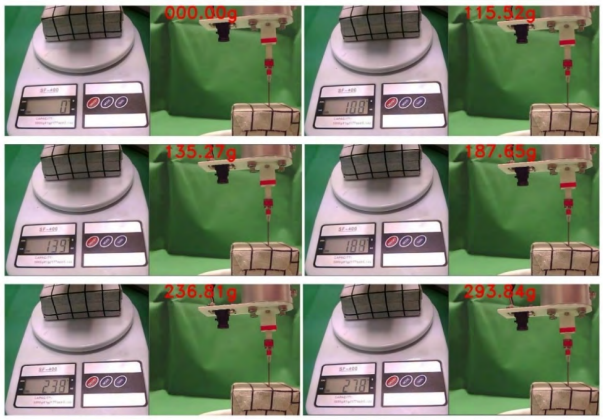

FIGURE 9. Results of the force estimation.

TABLE 2. Specific experimental data of the final frame.

Number	Actual value of the force (g)	Estimate value of the force (g)	Absolute error (g)
1	0	000.00	0.00
2	108	115.52	7.52
3	139	135.27	3.73
4	189	187.65	1.35
5	238	236.81	1.19
6	278	293.84	15.84
MAE			4.77

the object with different forces. The actual and estimated values of the force are shown in Fig. 9.

The results of force estimation are robust. The average error is $0.047N(4.77g)$, as shown in Table 2.

C. HAND-FORCE COORDINATION

Silica gel simulation skin is selected as the pressing object in hand-force coordination experiment, and its structure is shown in Fig. 10. The touching sensation is similar to that of real people.

The goal of hand-force coordination is to withdraw the needle when it hits the bone. The parameters are $k = 2, \alpha = \frac{1}{v}$, the speed of the needle is $0.25mm/s$, and the threshold of discrete force convolution is set to $3500g^2s/mm$. The above threshold value is used for the needle withdrawal experiment, as shown in Fig.11. In the experiment, as soon as the discrete force convolution is detected to exceed the threshold,

FIGURE 10. Artificial skin for press experiment.

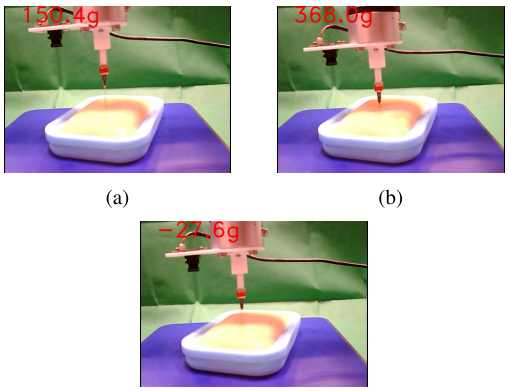

FIGURE 11. Periods of the withdrawal experiment. (a) Normal. (a) Hit the bone. (a) Withdraw.

the needle is immediately withdrawn at a maximum speed of $10mm/s$.

From the experimental results, it can be seen that the discrete convolution can well distinguish whether the needle hit the bone.

V. CONCLUSION

In this paper, a hand-eye-force coordination framework of acupuncture robot is proposed for the first time, which provides a theoretical basis for the research of acupuncture robot. We have shown that combining hand, eye, and force in the robot can complete the acupuncture task. Our method implements all three aspects of the acupuncture task: firstly, hand-eye coordination is leveraged to get the robot arm to the target position accurately; secondly, the magnitude of the force is estimated as a constraint relied on eye-force coordination; and thirdly, acupuncture is performed with the help of hand-force coordination, which ensures safety and reliability. In future work, we seek more flexible mechanical structures, more robust control methods, and more complex needling techniques. Endowing the acupuncture robot with the function of needling angle control to choose suitable angles of needling is also an interesting work.

REFERENCES

[1] P. Robertshawe and S. Dowie, "Acupuncture: An aid to differential diagnosis," *J. Austral. Traditional-Med. Soc.*, vol. 16, no. 2, pp. 108–109, 2010.
[2] H. Yamashita, H. Tsukayama, Y. Tanno, and K. Nishijo, "Adverse events related to acupuncture," *J. Amer. Med. Assoc.*, vol. 280, no. 18, pp. 1363–1364, 1998.
[3] N. Listed, "Acupuncture: National Institutes of Health Consensus Development Conference statement," *Dermatol. Nursing*, vol. 12, no. 2, p. 126, 2000.
[4] A. Taub, "Thumbs down on acupuncture," *Science*, vol. 279, no. 5348, p. 155, 1998.
[5] N. Goldman, M. Chen, T. Fujita, Q. Xu, W. Peng, W. Liu, T. K. Jensen, Y. Pei, F. Wang, X. Han, J.-F. Chen, J. Schnermann, T. Takano, L. Bekar, K. Tieu, and M. Nedergaar, "Adenosine A1 receptors mediate local antinociceptive effects of acupuncture," *Nature Neurosci.*, vol. 13, no. 7, p. 883, 2010.
[6] T. C. Xu and D. D. Lu, "Application and exploration of acupuncture robot in quantitative research of acupuncture," *J. Traditional Chin. Med.*, vol. 58, no. 9, pp. 752–755, 2017.
[7] S. Maeso, M. Reza, J. A. Mayol, J. A. Blasco, M. Guerra, E. Andradas, and M. N. Plana, "Efficacy of the da vinci surgical system in abdominal surgery compared with that of laparoscopy: A systematic review and meta-analysis," *Ann. Surgery*, vol. 252, no. 2, pp. 254–262, 2010.
[8] X. M. Du, Y. S. Zhang, "Advances in application of da vinci surgical system," *China Med. Equip.*, vol. 8, no. 5, pp. 60–63, 2011.
[9] D. Nio, W. A. Bemelman, K. T. Boer, M. S. Dunker, D. J. Gouma, and T. M. Gulik, "Efficiency of manual versus robotical (Zeus) assisted laparoscopic surgery in the performance of standardized tasks," *Surgical Endoscopy Interventional Techn.*, vol. 16, no. 3, pp. 412–415, 2002.
[10] M. Lefranc and J. Peltier, " Evaluation of the ROSA Spine robot for minimally invasive surgical procedures," *Expert Rev. Med. Devices*, vol. 13, no. 10, pp. 899–906, 2016.
[11] C. V. Riga, C. D. Bicknell, A. Rolls, N. J. Cheshire, and M. S. Hamady, "Robot-assisted fenestrated endovascular aneurysm repair (FEVAR) using the magellan system," *J. Vascular Intervent. Radiol.*, vol. 24, no. 2, pp. 191–196, Feb. 2013.
[12] P. Neuzil, S. Cerny, S. Kralovec, O. Svanidze, J. Bohuslavek, P. Plasil, P. Jehlicka, F. Holy, J. Petru, R. Kuenzler, and L. Sediva, "Single-site access robot-assisted epicardial mapping with a snake robot: Preparation and first clinical experience," *J. Robot. Surgery*, vol. 7, no. 2, pp. 103–111, Jun. 2013.
[13] Y. Wang and C. Zhao, "A new type of acupuncture robot," *Robot Techn. Appl.*, no. 4, pp. 37–39, 2007.
[14] X. T. Wang, *The Complete Book of Chinese Acupuncture*. Henan, China: Henan Science And Technology Press, 1992.
[15] F. Xu, K. S. Zheng, and Y. M. Huang, *A Complete Collection of Acupuncture and Moxibustion*. Beijing, China: People's Medical Publishing House, 1987.
[16] S. Hutchinson, G. D. Hager, and P. I. Corke, "A tutorial on visual servo control," *IEEE Trans. Robot. Autom.*, vol. 12, no. 5, pp. 651–670, Oct. 1996.
[17] S. W. Wijesoma, D. F. H. Wolfe, and R. J. Richards, "Eye-to-hand coordination for vision-guided robot control applications," *Int. J. Robot. Res.*, vol. 12, no. 1, pp. 65–78, 1993.
[18] E. Malis, F. Chaumette, and S. Boudet, "2 1/2 D visual servoing," *IEEE Trans. Robot. Autom.*, vol. 15, no. 2, pp. 238–250, Apr. 2002.
[19] B. Espiau, F. Chaumette, and P. Rives, "A new approach to visual servoing in robotics," *IEEE Trans. Robot. Autom.*, vol. 8, no. 3, pp. 313–326, Jun. 1992.
[20] E. C. Dean-Leon, V. Parra-Vega, A. Espinosa-Romero, and J. Fierro, "Dynamical image-based PID uncalibrated visual servoing with fixed camera for tracking of planar robots with a heuristical predictor," in *Proc. 2nd IEEE Int. Conf. Ind. Inform. (INDIN)*, Jun. 2004, pp. 339–345.
[21] J. A. Piepmeier, G. V. McMurray, and H. Lipkin, "Uncalibrated dynamic visual servoing," *IEEE Trans. Robot. Autom.*, vol. 20, no. 1, pp. 143–147, Feb. 2004.
[22] S. Levine, P. Pastor, A. Krizhevsky, J. Ibarz, and D. Quillen, "Learning hand-eye coordination for robotic grasping with deep learning and large-scale data collection," *Int. J. Robot. Res.*, vol. 37, nos. 4–5, pp. 421–436, 2017.
[23] J. Žunić, K. Hirota, and P. L. Rosin, "A Hu moment invariant as a shape circularity measure," *Pattern Recognit.*, vol. 43, no. 1, pp. 47–57, Jan. 2010.
[24] J. F. Henriques, R. Caseiro, P. Martins, and J. Batista, "High-speed tracking with kernelized correlation filters," *IEEE Trans. Pattern Anal. Mach. Intell.*, vol. 37, no. 3, pp. 583–596, Mar. 2015.
[25] D. I. Kosmopoulos, "Robust Jacobian matrix estimation for image-based visual servoing," *Robot. Comput.-Integr. Manuf.*, vol. 27, no. 1, pp. 82–87, Feb. 2011.

JIANBO SU received the B.Sc. degree in automatic control from Shanghai Jiao Tong University, Shanghai, China, in 1989, the M.Sc. degree in pattern recognition and intelligent system from the Institute of Automation, Chinese Academy of Science, Beijing, China, in 1992, and the Ph.D. degree in control science and engineering from Southeast University, Nanjing, China, in 1995. He joined the Faculty of the Department of Automation, Shanghai Jiao Tong University, in 1997, where he has been a Full Professor, since 2000. His research interests include robotics, pattern recognition, and human machine interaction. He is a member of the Technical Committee of Networked Robots, the IEEE Robotics and Automation Society, a member of the Technical Committee on Human Machine Interactions, the IEEE System, Man, and Cybernetics Society, and a Standing Committee Member of the Chinese Association of Automation. He has been an Associate Editor for the IEEE TRANSACTIONS ON CYBERNETICS, since 2005, with which he received the Best Associate Editor Award from the IEEE SMC society, in 2014.

YICHENG ZHU received the B.Eng. degree in automation from Southeast University, Nanjing, China, in 2018. He is currently pursuing the M.Sc. degree with the Department of Automation, Shanghai Jiao Tong University, Shanghai, China. His current research interests include robot control and reinforcement learning.

MINGDE ZHU received the B.Sc. degree in automation and the M.Sc. degree from Shanghai Jiao Tong University, Shanghai, China, in 2015 and 2018, respectively. His current research interests include service robots and pattern recognition.